Europhys. Lett., **39** (6), pp. 617-622 (1997)

Ordering and viscoelastic relaxation in multiarm star polymer melts

D. Vlassopoulos[1], T. Pakula[2], G. Fytas[1]
J. Roovers[3], K. Karatasos[1] and N. Hadjichristidis[1]

[1] *FORTH, Institute of Electronic Structure & Laser*
P.O. Box 1527, 71110 Heraklion, Crete, Greece
[2] *Max Planck Insitut für Polymerforschung - Postfach 3148, D-55021 Mainz, Germany*
[3] *National Research Council - Ottawa, Ontario K1A 0R6, Canada*

(received 25 April 1997; accepted in final form 30 July 1997)

PACS. 61.25Hq – Macromolecular and polymer solutions; polymer melts; swelling.
PACS. 61.41+e – Polymers, elastomers, and plastics.
PACS. 61.10Eq – X-ray scattering (including small-angle scattering).

Abstract. – We present small-angle X-ray scattering measurements in model star homopolymer melts with high functionality, revealing liquid-like ordering. Monte Carlo simulations attribute this structure to the nonuniform intramolecular segmental mass distribution, which results in core-shell topology. This ordering is also reflected in their linear viscoelastic response as a new structural mode at low frequencies, due to cooperative rearrangements of the stars.

Polymer stars constitute a special case of tethered chains, in which linear macromolecules are attached by one end to a central core. In the simplest case of a single star in a good solvent, when the number of arms, f, is high, the segment density near the core is much higher than in the periphery, as described by the model of Daoud and Cotton [1] and confirmed in block copolymer micelles by small-angle neutron scattering (SANS) experiments [2]; such a multiarm star polymer can be considered as a prototype spherical brush with soft colloidal character (core-shell structure) [3], [4]. Stars of low functionality (typically $f < 32$) have been extensively studied both in solution and in the melt, theoretically and experimentally [4]. Their dynamics is essentially governed by arm relaxation, with f-independent zero shear viscosity $\eta_0 \sim \tau_a \sim \exp[\alpha M_a]$, where τ_a the arm relaxation time, M_a the arm molecular weight and $\alpha \simeq 0.6$ [5]. In contrast, multiarm stars ($f = 64$ or 128) which have been synthesized only recently [6], have received much less attention, despite their potentially rich morphology and dynamics in solution or in the melt. So far, investigations have been carried out exclusively in solution. In good solvent around the overlap concentration, these stars order in a macrolattice due to the increased osmotic pressure [7], as shown by SANS [8] and predicted by scaling arguments [9]. Diblock copolymer micelles exhibit similar self-assembling features [10]. Despite these developments, however, the static conformation of multiarm star polymer *melts* has been virtually unexplored. Yet, in analogy to the semi-dilute solutions and in view of the observed

TABLE I. – *Molecular characteristics and relaxation times (at −83 °C) of model star polymers.*

Code	f	M_a	τ_a(s)	τ_c(s)
PB(linear)	2	77,500	2.74×10^6	—
4S	4	10,900	8.67×10^3	—
6407	62	6,330	791	1.28×10^4
12807	124	6,800	1000	1.04×10^5
12814	125	13,000	2.81×10^4	1.81×10^6

deviation from the η_0 scaling for melts with $f = 32$ [11], the investigation of the potential structure formation in the latter and its manifestation in the viscoelastic response, is necessary.

In this letter we present experimental evidence of ordering in multiarm star homopolymer melts, which is a consequence of their inherent macromolecular excluded volume. This liquid-like ordering is also reflected in their linear viscoelastic response.

The model polybutadiene (PB) star polymers used in this study are listed in table I, along with their molecular characteristics (M_a, f) and relaxation times (discussed below); they have been prepared by coupling anionically synthesized narrow molecular-weight distribution (< 1.1) linear polyPBs (arms) with small carbosilane dendritic coupling agents, constituting highly branched star centers of different generations, depending on the desired functionality [6].

Based on the synthesis and molecular structure of the multiarm stars, due to the difference in chemical constitution between the center and the arms, and the resulting electron density contrast, small-angle X-ray scattering (SAXS) is a particularly suitable tool for studying the structure of these systems. Measurements were carried out at room temperature in vacuum. Typical results of the X-ray scattered intensity distribution for two melts with $f = 128$ are depicted in fig. 1. Each measurement was performed on a bulk sample by means of a Kratky compact camera equipped with a one-dimensional position-sensitive detector. The scattered

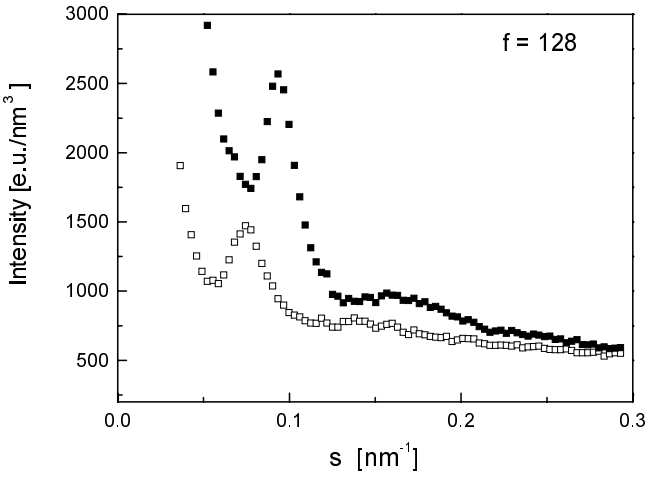

Fig. 1. – Scattering intensity profile of star melts 12807 (■) and 12814 (□) from SAXS (wavelength $\lambda = 0.154$ nm) at 20 °C.

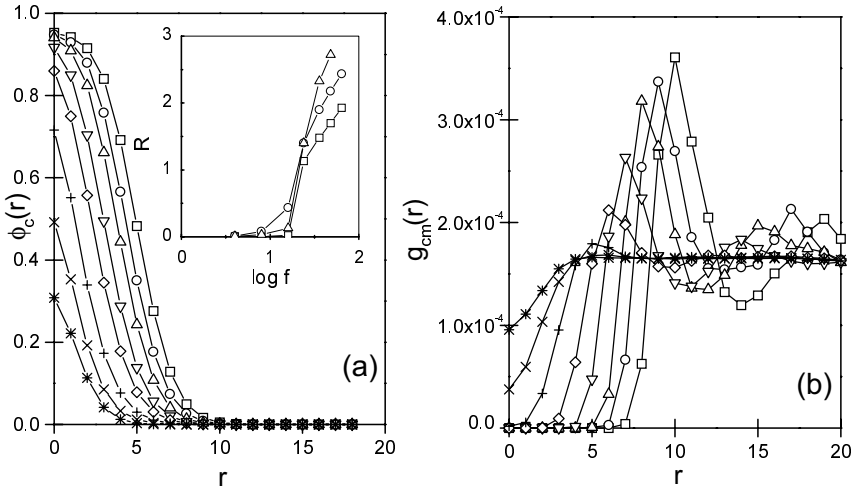

Fig. 2. – Characteristics of the structure in the simulated melt of star molecules: a) distributions of intrastar density of a single star around the center of mass with $N_a = 20$ and varying f (□ $f = 64$; ○ $f = 48$; △ $f = 36$; ▽ $f = 24$; ◇ $f = 16$; + $f = 8$; × $f = 4$; ∗ $f = 2$). Inset: core radius R as a function of N_a (□ $N_a = 10$; ○ $N_a = 20$; △ $N_a = 40$) and f. b) Center-of-mass pair correlation functions.

intensity was corrected for absorption, background scattering and slit-length smearing. In both samples 12807 and 12814, which differ only in the arm length, intense peaks are observed with maximum intensities at $s_{max} = q/2\pi = 0.094$ nm^{-1} and 0.074 nm^{-1}, respectively (q is the scattering wave vector). Much less intense higher-order maxima can be seen at higher s values, approximately at positions $\sqrt{3}$ and $\sqrt{7}$ with respect to the position of the first intense peak. This indicates a structure of an ordered liquid state, such as that observed in liquid mercury [12]. The positions of the higher-order maxima can suggest an fcc lattice, but their low intensities indicate that this type of order is only weakly developed. The distances between nearest-neighboring star centers are estimated from $d = a/s_{max}$, where $a = 1.22$ for an fcc lattice or 1.23 for a structure controlled only by two-body correlations [12]. Using the latter value, we obtain $d = 13.1$ nm and 16.6 nm for 12807 and 12814, respectively. In a dense system such as a polymer melt, the same values can be regarded as an approximation of star sizes and should satisfy the relationship $d \sim M_a^{1/3}$, which they do satisfactorily.

Further, a crude estimation of the ratio of peak heights of 12807 over 12814, without interpenetration, is 2, in reasonable agreement with the experimental value of 1.7 from fig. 1.

A strong supporting evidence of ordering and hint at its origin comes from computer simulations of corresponding model systems. They were performed using the cooperative motion algorithm (CMA), which is suitable for dense systems of well-defined topologically complex molecular objects [13]. Ensembles of beads on an fcc lattice were connected by non-breakable bonds into objects representing macromolecules of a specific topology. Systems with star polymers with 10–40 repeat units per arm (N_a) and $f = 2$–64 were considered. Model systems consisting of 30000 beads were simulated. Initially, an ordered star configuration was "melted" (randomized) and equilibrated in athermal conditions. Considering fast relaxation of star shapes and strong distance correlations only between nearest neighbours ensured that equilibrium had been reached. To characterize the structure, the intrastar mass distribution of beads around the center of mass of stars, $\Phi_c(r)$, and the pair correlation functions of the star centers of mass, $g_{cm}(r)$, were calculated. Typical examples for $N_a = 20$ and various f

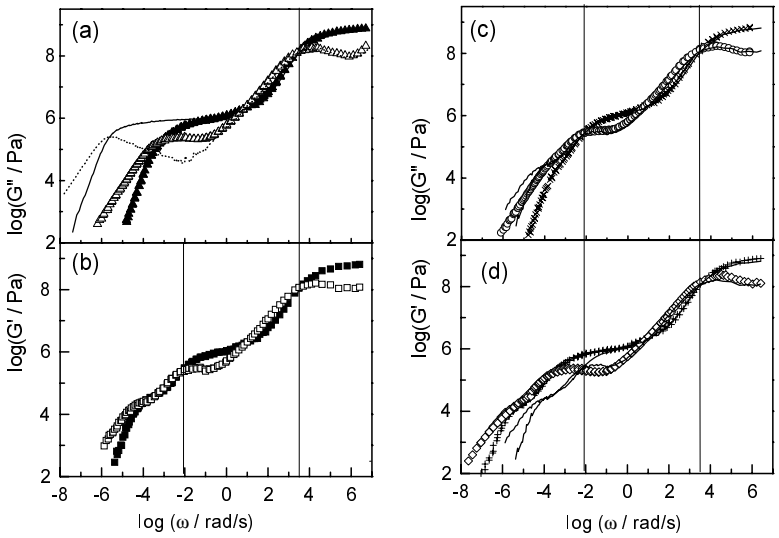

Fig. 3. – Master curves of elastic (G') and viscous (G'') moduli in the range −103 °C–60 °C, with reference temperature −83 °C: a) linear PB (G': solid line; G'': dashed line) and $f = 4$ star (G': ▲; G'': △); b) 12807 (G': ■, G'': □); c) 12807 (solid lines) and 6407 (G': ×, G'': ○); d) 12807 (solid lines) and 12814 (G': +, G'': ◇). Vertical lines indicate the f-independence of arm relaxation (low-frequency regime) and the insensitivity of segmental relaxation to both f and M_a (high-frequency regime).

are shown in fig. 2. A strong influence of f on the structure of a single star (fig. 2 a)) and on the structure of the whole system, *i.e.* the melt (fig. 2 b)), is indicated. The maximum intrastar density within stars with $f < 16$ is considerably smaller than the average density of the system, whereas for stars with $f \geq 16$ the density at the star center approaches the nominal density of the system. This means that stars with smaller f interpenetrate each other, but when $f \geq 16$ the centers of stars become practically impenetrable for elements of other stars. The latter effect causes strong spatial correlation of the stars centers with respect to the neighbours, as indicated by the distinct maxima in the $g_{cm}(r)$ of fig. 2 b). Stars seem to separate into two categories, those without core ($f < 16$) and those with a core ($f > 16$); this distinction is only of qualitative value and shows the ability of simulations to capture the main physics. This effect is also illustrated in the inset of fig. 2 a) by means of dependences of the core size, R, on f for various N_a; core sizes have been determined by an analysis of single-star density distributions [14]. Comparing simulations and experiments, the former do not account for polydispersity in f, and consider as segmental length $\alpha\sqrt{2}$ with α the lattice constant. Given these differences, the results show that for star melts with $f > 16$ an ordering of star positions should be observed as a result of the "excluded-volume effect" taking place on the macromolecular size scale.

To examine the effects of this ordering on the dynamics of the stars, small-amplitude oscillatory shear measurements were carried out by means of Rheometric Scientific RMS-800 and ARES mechanical spectrometers in the parallel plate geometry (diameter 8 mm, gap 0.7 mm), air convection temperature control and N_2 atmosphere, in a wide temperature range (−103 °C–60 °C). Figure 3 depicts master curves of elastic (G') and viscous (G'') moduli with reference temperature −83 °C.

In fig. 3 a) the behaviour of long linear PB chains and 4-arm stars (4S) is illustrated for comparison. In both cases two well-distinguishable relaxation processes are observed as

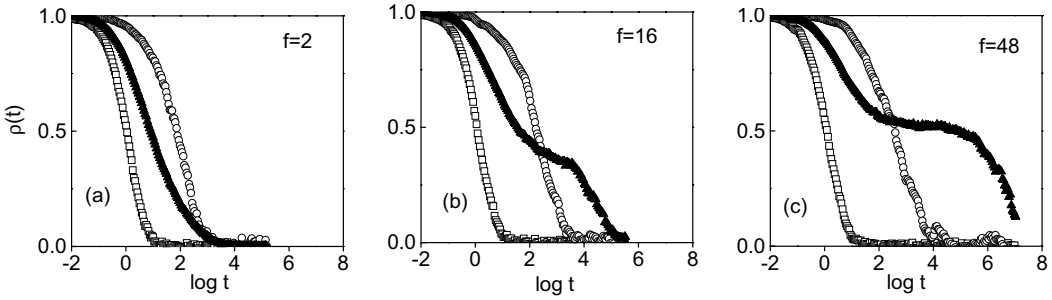

Fig. 4. – Autocorrelation functions of simulated star melts with $N_a = 20$ and $f = 2$ (a), 16 (b), 48 (c): □ segment position, $\rho_s(t)$; ○ center-to-end vectors of arms, $\rho_R(t)$; ▲ positions of star elements, $\rho_c(t)$.

expected: the high-frequency relaxation, attributed to the segmental motion (the α-primary glass-rubber process), and the low-frequency relaxation, attributed to orientational motion of linear chains or star arms (terminal process) [13], [5]. Figures 3 b)-d) depict results for melts of multiarm stars. The segmental relaxation is virtually unaffected by the change of f or N_a, as indicated by the vertical line. A striking effect of the increase of f is, however, observed in the terminal region. Instead of a single relaxation (as in the cases of fig. 3 a)), the transition from the plateau range to the Newtonian flow regime of the multiarm star melts takes place in two steps, indicating two well-separated relaxation processes. The best example observed is shown in fig. 3 b), for 12807 with high f and small N_a. In fig. 3 c) 12807 is compared with 6407; it is observed that the change of f influences only the low-frequency mode of the terminal relaxation (with characteristic time τ_c). In fig. 3 d), on the other hand, 12807 is compared with 12814; in this case the change of N_a for the same f influences considerably both relaxation modes of the terminal region by shifting them nearly parallel to lower frequencies. From the relaxation times determined for all systems (table I), it is clear that the high-frequency relaxation of the terminal regime can be attributed to the orientational relaxation of star arms, depending on M_a and not on f (vertical line in figs. 3 b)-d)). The slower terminal process is only observed in systems with high f, and its separation from the high-frequency mode depends on f; we attribute this process to a structural relaxation apparent only in star melts, exhibiting a distinct order. A similar extra relaxation at low frequencies was also observed in self-assembling block copolymer micelles and attributed to ordering [15].

The dynamics in simulated systems representing multiarm star melts was monitored via various correlation functions. Local dynamics in model systems was characterized by the segment position autocorrelation function $\rho_s(t)$, relaxation of star arms is described by the autocorrelation function of the center-to-end vectors of arms $\rho_R(t)$ and the motion of the whole stars is observed as the autocorrelation of positions of all star elements $\rho_c(t)$ [13]. Figure 4 depicts typical examples of these correlation functions for stars with constant $N_a = 20$ and different f. It is noted that in all systems, independently of f, the segmental relaxation is the same, which is consistent with the experiments (fig. 3). Results in fig. 4 a) describe the behaviour of linear chains ($f = 2$). In this case the dynamics is mainly controlled by the orientational relaxation of the chain, which essentially contributes to the relaxation of the center-to-end vector. The broad chain position correlation includes many motion modes which range between fast local conformational changes and slower global chain translations, all contributing to displacements of the chain with respect to its original (at $t = 0$) contour. The situation changes considerably when the number of arms in the star becomes high. Whereas the arm relaxation changes only slightly with the increase of f (in agreement with the behaviour

of a single star in a good solvent [16]), the position correlation of stars becomes long-living, with the slow component of this relaxation considerably exceeding the relaxation time of the arms. The faster component of the star position correlation reflects arm motions at the star periphery and can be attributed to a form relaxation of the stars (as deformable objects), but for stars with large f, which almost completely fill the space around the mass center, a complete relaxation must be related to the translational motion of the whole star by a distance comparable to the star size. Therefore, the slow component of the position correlation is attributed to a translational motion of the stars beyond the originally occupied space, a process which in ordered systems can only take place cooperatively with some neighbours. This type of relaxation exceeds the size scale of a single star and therefore becomes the slowest mode in the system. These results reflect a dynamic behaviour which is in good qualitative agreement with the experimental observations (fig. 3), and thus support the assignment of the modes of the terminal relaxation, detected by linear viscoelastic measurements.

From the above results, we conclude that melts of multiarm stars constitute a special class of macromolecular systems in which properties of simple liquids are reflected on the macromolecular scale. Both the molecular order and the nature of relaxation determining the Newtonian flow range of these systems seem to have features which are normally attributed to simple molecular liquids.

In summary, it has been shown that multiarm star homopolymers order in the melt, as a consequence of the strong position correlation of their impenetrable centers. This ordering is manifested in the linear viscoelastic relaxation of these model spherical brushes.

REFERENCES

[1] Daoud M. and Cotton J. P., *J. Phys.* (*Paris*), **43** (1982) 531.

[2] Förster S., Wenz E. and Lindner P., *Phys. Rev. Lett.*, **77** (1996) 95.

[3] Halperin A., Tirrell M. and Lodge T., *Adv. Polym. Sci.*, **100** (1992) 31.

[4] Grest G. S., Fetters L. J., Huang J. S. and Richter D., *Adv. Chem. Phys.*, **XCIV** (1996) 65.

[5] Ball R. C. and McLeish T. C. B., *Macromolecules*, **22** (1989) 1911; Milner S. T. and McLeish T. C. B., *Macromolecules*, **30** (1997) 2159 Fetters L. J., Kiss A. D., Pearson D. S., Quack G. F. and Vitus F. J., *Macromolecules*, **26** (1993) 647.

[6] Roovers J., Zhou L. L., Toporowski P. M., Van Der Zwan M., Iatrou H. and Hadjichristidis N., *Macromolecules*, **26** (1993) 4324.

[7] Roovers J., Toporowski P. M. and Douglas J., *Macromolecules*, **28** (1995) 7064.

[8] Richter J. D., Jucknischke O., Willner L., Fetters L. J., Lin M., Huang J. S., Roovers J., Toporowski C. and Zhou L. L., *J. Phys. IV*, **3** (1993) C8, 3; Willner L., Jucknischke O., Richter D., Farago B., Fetters L. J. and Huang J. S., *Europhys. Lett.*, **19** (1992) 297.

[9] Witten T. A., Pincus P. A. and Cates M. S., *Europhys. Lett.*, **2** (1986) 137.

[10] McConnell G. A., Gast A., Huang J. and Smith S., *Phys. Rev. Lett.*, **71** (1993) 2102; Gast A. P., *Langmuir*, **12** (1996) 4060.

[11] Roovers J., *Macromolecules*, **24** (1991) 5895.

[12] Guinier A., *X-Ray Diffraction* (Freedman, San Francisco) 1963.

[13] Pakula T., Geyler S., Edling T. and Boese D., *Rheol. Acta*, **35** (1996) 631.

[14] Pakula T. *et al.*, unpublished results.

[15] Sato T., Watanabe H., Osaki K. and Yao M.-L., *Macromolecules*, **29** (1996) 3881.

[16] Grest G. S., Kremer K., Milner S. T. and Witten T. A., *Macromolecules*, **22** (1989) 1904; Boese D., Kremer F. and Fetters L. J., *Macromolecules*, **23** (1990) 1826.